Studies on Water-Gas-Shift Enhanced by Adsorption and Membrane Permeation

F.R. García-García[1], M. León[2], S. Ordóñez[2]and K. Li[1*]

[1]Department of Chemical Engineering and Chemical Technology, ImperialCollegeLondon, South Kensington Campus, LondonSW7 2AZ, UK

[2]Department of Chemical and Environmental Engineering, University of Oviedo, Julián Clavería s/n, 33006 Oviedo, Spain

ABSTRACT

A new sorption enhanced membrane reactor (SEMR), consisting of a packed adsorbent-catalyst bed (10% CuO/CeO_2 catalyst and a hydrotalcite-derived Mg-Al mixed oxide) around a tubular Pd/Ag hollow fibre membrane, has been proposed to obtain high purity H_2 and simultaneous capture of CO_2 during the water gas shift reaction. For comparison purposes, catalytic activity tests were carried out at atmospheric pressure and operating temperatures between 100^{o}C and 550^{o}C in three different catalytic reactors: (1) a fixed-bed reactor (FBR), (2) a sorption enhanced reactor (SER) and (2) a new SEMR. In all cases, the feed mixture Ar/CO/H_2O ratio was 11/1/0.75 with a space velocity of 22 L/g·h. The performance of the FBR was used as a reference to compare with the results obtained from the SER and SEMR. The H_2 yield at 350ºC using the SER was 80%, which is 33% higher than that obtained in the traditional FBR and 18% higher than the corresponding thermodynamic equilibrium. However, due to the high CO/H_2O ratio (R > 1), undesirable side-reactions such as C deposition become important at temperatures higher than 400ºC. A similar behaviour was observed using the SEMR, however in this case, a high purity CO_x free H_2 production was obtained. This preliminary study shows relevant data obtained using a SER and the new SEMR, which allows for the better understanding and design of multifunctional catalytic reactors.

*To whom correspondence should be addressed:

Tel: 44 (0) 207-5945676. Fax. 44 (0) 207-5945629. E-mail address: kang.li@imperial.ac.uk

1. Introduction

The transition from current brown hydrogen economy to a green economy is set to occur in upcoming decades [1,2]. However, in the meantime, efforts must be focused on making this transition as environmentally friendly as possible [3,4]. Today,96% of the global H_2 production is based on steam reforming of fossil fuels followed by the water gas shift (WGS) reaction, which produces about 250 million tons per year of CO_2 [5, 6]. At this point, membrane and sorbent technologies are the growing interest in scientific community due to their potential for controlling and managing CO_2 emissions. The development of H_2-selective inorganic membranes, such as Pd-based membranes, allows not only the production of high purity H_2 from fossil fuels but also capture the CO_2 in a subsequent step [7]. Likewise, the synthesis of new materials such as lithium ceramics, hydrotalcites and calcium-based materials allow in-situ capture of CO_2 at a wide range of temperatures [8].

Pd-based membranes are extensively studied, either for H_2 separation/purification or reaction processes, due to its advantages over the traditional technologies. Compared to traditional fixed-bed reactors (FBR), catalytic membrane reactors (CMR), combining an active catalyst and an H_2 permselective membrane in a single unit, have demonstrated their enhanced performance in different processes and under a wide range of reaction conditions [9-10]. In this respect, the attractive physical and chemical properties of ceramic hollow fibres along with their low-cost manufacturing process suggest them as the key step for suitable intensification of today heterogeneous catalytic gas phase process [11-14]. It has been demonstrated that the higher surface area/volume ratio of the ceramic hollow fibres in comparison with the convectional ceramic or stainless steel tubular supports results in a more efficient use of the membrane deposited on its outer surface. Moreover, a hollow fibre membrane reactor (HFMR), which consists of a packed catalyst bed around a Pd-based

coated ceramic hollow fibre membrane permits the reduction of the amount of Pd wasted in a CMR and to decrease significantly the final volume size of the reactor. Among the existing Pd-based membranes, the physical and chemical properties of the Pd/Ag alloy membranes make them suitable candidates for these applications. First, Pd/Ag alloy membranes show higher H_2 permeability than Pd membranes in a temperature range of 150-450 ºC due to their higher H_2 solubility [15, 16]. Secondly, the melting point of the Pd/Ag alloys is higher than that of pure Pd, which increases their sintering resistance and enables them to work at higher temperatures than Pd membranes [17]. Finally, the fact that Pd/Ag alloy membranes do not show an α-β phase transition makes them resistant to embrittlement at temperatures below 300 °C [18, 19].

Another procedure for shifting the equilibrium consists of blending the catalyst with a CO_2 adsorbent, so-called sorption-enhanced fixed bed reactors (SER). In this case the equilibrium shift is accomplished by the selective removal of one of the reaction products (CO_2). Several examples of successful SERs have already been reported in the literature for other reactions [20-23]. For this purpose, an ideal CO_2 sorbent should exhibit high capture capacity, durability, fast capture/release kinetics and good mechanical strength. In this respect, hydrotalcites show fast kinetics and high CO_2 capture capacity in the temperature range of 200-500 ºC in addition to maintaining a high stability during cyclic carbonation [24, 25].

It is important to mention the advantages of using either CMR and SER over traditional FBR. First, they present the possibility of working at significantly lower temperatures and/or using lower amounts of catalyst. Secondly, they combine the processes of generating and separating H_2 or capture CO_2 in a single step, which is possible due to either the high H_2 selectivity of the Pd-base membrane or the high CO_2 selectivity of the sorbent. Finally, they overcome thermodynamic limitations by selectively removing one of the products from the

reaction medium, which shifts the equilibrium to the products side according to Le Chatelier's principle.

The integration of both membrane and sorbent technologies is a critical step for process intensification of the WGS reaction: $CO + H_2O \rightarrow CO_2 + H_2$. Since the early 1960s [26], the WGS reaction has been performed in industry as a three-stage process. In the first stage, the CO reacts with H_2O to produce CO_2 and H_2 in a high temperature (HT) reactor. In the second stage, the remaining CO (0.1% Vol) is oxidized in a low temperature (LT) reactor. Finally, H_2 and CO_2 are separated in a separation unit, which usually consists of a selective adsorbent bed. Even though a lot of work has been done to optimize each of these stages, a three-stage process is less economically feasible than a single-stage process. In this regard, integrating the whole process into a single-stage process by using a sorbent enhance membrane reactor (SEMR) could significantly decrease the cost of H_2 production compared with the current three-stage process.

The concept of the SEMR, which integrates both a packed adsorbent-catalyst bed and a selective membrane in a single reactor, was originally proposed by B. Park and T.T. Tsotsis in 2001 [27-29]. In their study [27], they reported the performance in esterification reactions of a so-called hybrid adsorbent-membrane reactor (HAMR) system, which combined a water-permeable polymeric membrane and a hydrophilic adsorbent in one unit. The HAMR shows several advantages over either CMR or SER. First, the HAMR system allows for higher conversion and yields than that obtained in either CMR or SER along with a maximum selectivity. In addition, the operational flexibility of the HAMR system enables in situ regeneration of the selective adsorbent under reaction conditions. The potencial applications of both HAMR [30, 31] and circulating fluidized-bed HAMR [32-35] systems for hydrogen production by methane steam reform and water gas shift reactions have recently been studied. However, the number of publications in this area is still limited.

For these reasons, the goal of this work is to develop a novel SEMR, which integrates both a SER and CMR in a single unit. The original configuration of the SEMR allows continuous high purity H_2 production together with in situ CO_2 capture in the WGS reaction. The performance of the SEMR was compared with that of both FBR and SER. Three different parameters (i.e., catalytic activity, H_2 permeability of the Pd/Ag alloy membrane and CO_2 adsorption on the hydrotalcite under the WGS reaction conditions) were studied in order to optimize the performance of the SEMR.

2. Experimental

1. Synthesis of the 10%CuO/CeO_2 catalyst

The 10% CuO/CeO_2 catalyst was prepared using the sol-gel Pechini method. $Ce(NO_3)_3.6H_2O$ (99.0% Fluka Analytical) and $Cu(NO_3)_2.3H_2O$ (99% Acros Organic) were dissolved in 50 ml deionised water. The amount of $Ce(NO_3)_3.6H_2O$ and $Cu(NO_3)_2.3H_2O$ were calculated for a 10 % CuO loading. After both metal nitrates were fully dissolved, citric acid (99.0% Sigma-Aldrich) was added to the solution with a molar ratio of 2:1 of citric acid to metal ions. The process was continued by adding ethylene glycol to the solution such that the molar ratio between citric acid and ethylene glycol was 1:1.2. The catalyst solutions were kept stirring for 3 hours and later placed in an oven (SalvislabThermocenter) for drying at 115^{o}C for 24 hours to form a foamy dry gel. The dry gel was then calcined in a tubular furnace (Vecstar Furnaces, VCTF/SP) at 400^{o}C for an hour. Information about the characterization of the 10% CuO/CeO_2 catalyst can be found elsewhere [36].

2. Synthesis of hydrotalcite-derived Mg-Al mixed oxides

A hydrotalcite with a Mg/Al ratio of 3 was synthesized by coprecipitation at low supersaturation conditions and under sonication. 1 mol/L solutions of $Mg(NO_3)_2 \cdot 6H_2O$ (Fluka, >99%) and $Al(NO_3)_3 \cdot 9H_2O$ (Panreac, 98%) were mixed in a 3:1 molar ratio. A volume of 150 mL of this solution was added drop-wise to 100 mL of 0.2 M K_2CO_3 (Panreac, 99%) under vigorous stirring and ultrasound irradiation at room temperature. The pH was kept at 10 by adding appropriate quantities of 1.6 M NaOH (Prolabo, 98%) solution. The precipitate was then separated by high-speed centrifugation, washed in deionized water in order to remove the alkali metals and the nitrate ions to a pH of 7, and dried in an oven at 100 ºC for 24 h. The resulting hydrotalcite was calcined at 450ºC under air flow for 7 h to obtain the mixed oxide. Further details on the preparation procedure are given in [31].

3. Fabrication of Al_2O_3 hollow fibres

Asymmetric Al_2O_3 hollow fibres were prepared using 1 μm, 0.3 μm, 0.05 μm and 0.01 μm Al_2O_3 powders (from Alfa Aesar), polyethersulfone (Radal A300, Ameco Performance), N-methyl-2-pyrrolidone (HPLC grade) and Arlacel P135 (Polyethyleneglycol 30-dipolyhydroxystearate, Uniqema) using a phase-inversion technique, followed by sintering at high temperatures. A detailed procedure for the synthesis of these hollow fibres can be found elsewhere [37].

4. Fabrication of the Pd/Ag membrane

The synthesis of the Pd/Ag membranes requires ammonium tetrachloropalladate, ($Pd(NH_4)_2Cl_4$, 99.99 %, Aldrich), palladium chloride ($PdCl_2$, 99.999%, Aldrich), tin chloride ($SnCl_2 \cdot 2H_2O$, Fisher Sci. Ltd.), ethylenediaminetetraacetic acid ($Na_2EDTA \cdot 2H_2O$, Fisher Sci. Ltd.), hydrochloric acid (HCl, 37 %, Fisher Sci. Ltd.), hydrazine (N_2H_4, Fisher Sci. Ltd.),

silver nitrate ($AgNO_3$, 99.99 %, Fisher Sci. Ltd.) and ammonium hydroxide ($NH_3 \cdot H_2O$, 28 %, Fisher Sci. Ltd.)

Prior to coating the Pd/Ag membrane, the outer surface of the Al_2O_3 hollow fibre was coated with a thin and gas-tight layer of white glaze in order to block the pores in the coated area; only 10 cm in the central part of the Al_2O_3 hollow fibre were left uncoated where the Pd/Ag membrane was deposited by electroless plating technique. Before the activation process, the Al_2O_3 hollow fibres were cleaned using deionised water and subsequently activated by sequential dipping in $SnCl_2$-HCl (1g/L, pH:2) and in $PdCl_2$-HCl (1g/L, pH:2) solutions. The activation process was repeated six times, after which the surface colour of the Al_2O_3 hollow fibre changed from white to dark brown. The Al_2O_3 hollow fibres activated with Pd seeds were then coated with Pd/Ag using sequential multi-layer electroless plating technique. During the preparation of the Pd/Ag membrane, the Pd layer was deposited first and then the Ag layer, since the ability of Pd to penetrate the pores of the support is higher than Ag and high metal to ceramic adhesion can be expected [38]. The resulting Pd/Ag membrane was dried in an oven at 120^{o}C for 2 hours (Memmert) before annealing in an H_2 atmosphere for 24 h at 400°C to obtain a uniform Pd/Ag alloy membrane.

5. Sorbent Enhanced Reactor (SER) configuration

A sorbent enhance reactor (SER) consists of a packed bed reactor where the catalyst has been blended with a selective adsorbent. A schematic representation of both a traditional fixed-bed Reactor (FBR) and the SER is shown in Figure 1. The SER integrates H_2 production and CO_2 capture in a single step. The CO_2 adsorption index, which represents the ability of the hydrotalcite to remove the CO_2 from the reaction medium under the WGS reaction conditions is defined as follows:

$$CO_2\ adsorption\ index(\%) = \frac{F_{CO_2}^{Adsorbed}}{F_{CO_2}^{Adsorbed} + F_{CO_2}^{Non-adsorbed}} \times 100\% \quad (1)$$

Where $F_{CO_2}^{Adsorbed}$ and $F_{CO_2}^{Non-adsorbed}$ are the molar flowrates of CO_2 adsorbed and non-adsorbed by the hydrotalcite, respectively. Whereas $F_{CO_2}^{Non-adsorbed}$ is measured on-line by using a gas chromatographer, $F_{CO_2}^{Adsorbed}$ is calculated according to the equation (2):

$$F_{CO_2}^{\text{Adsorbed}} = F_{H_2}^{Total} - F_{CO_2}^{\text{Non-adsorbed}} \quad (2)$$

Where $F_{H_2}^{Total}$ corresponds with the total molar flow rate of H_2 produced during the WGS reaction, and was measured on-line using a gas chromatograph. Finally, coke formation or yield to C during the WGS reaction ($Y_{C/CO}$) was calculated as follows:

$$Y_{C/CO} = ((F_{CO}^{\text{Intial}} - F_{CO}^{\text{Final}}) - F_{H_2}^{Total}) / F_{CO}^{Inital} \quad (3)$$

Where F_{CO}^{Intial} and F_{CO}^{Final} are the initial and final molar flow rates of CO measured on-line in a gas chromatographer, respectively.

6. Sorbent Enhance Membrane Reactor (SEMR) configuration

A schematic representation of the Sorbent Enhanced Membrane Reactor (SEMR), which consists of a packed adsorbent-catalyst bed around a Pd/Ag membrane coated on the outer layer of an Al_2O_3hollow fibre, is shown in Figure 1. In operation of the SEMR, a hydrotalcite was used for the removal of CO_2 whereas the removal of H_2 from the reaction zone was carried out using a co-current flow of Ar as a sweep gas to create a concentration gradient across the Pd/Ag-based membrane. The CO_2 adsorption index and coke formation under the WGS reaction conditions was calculated using equations 1 and 3, respectively. The

H_2recovery index, which represents the ability of Pd-based membranes to perform H_2 permeation is defined as follows:

$$H_2 \text{ recovery index (\%)} = \frac{F_{H_2}^{Permeate}}{F_{H_2}^{Permeate} + F_{H_2}^{Retentate}} \times 100\% \quad (4)$$

Where $F_{H_2}^{Permeate}$ and $F_{H_2}^{Retentate}$ represent the molarflow rate of H_2 across the Pd/Ag membrane and in the shell during the WGS reaction, respectively. Both, $F_{H_2}^{Permeate}$ and $F_{H_2}^{Retentate}$ were measured on-line by using a gas chromatograph. The total flow rate of H_2 produced during the WGS reaction was calculated as follows:

$$F_{H_2}^{Total} = F_{H_2}^{Permeate} + F_{H_2}^{Retentate} \quad (5)$$

7. Water Gas Shift reaction (WGS) catalytic studies

The catalytic activity of the 10% CuO/CeO_2 catalyst on the WGS reaction was studied in a conventional fixed-bed reactor, a sorbent enhance reactor and the sorbent enhance membrane reactor operating under atmospheric pressure over a temperature range from 100ºC to 500ºC. In all tests 35 mg of 10% CuO/CeO_2 catalyst were employed. The catalyst was diluted either in 2 g of SiC (FBR) or 3 g of Mg-Al mixed oxide (SER and SEMR). The feed mixture in all cases contained Ar (86.3%, molar base), CO (7.8%) and H_2O vapour (5.8%) which was supplied to the reactor by flowing 50 ml of Ar through a glass bubbler containing deionized water at 46^{o}C. The WGS reactions were carried out at a space velocity of 22 L/g.h and the total flow rate was 6 L/h, being the vumetric flow rates measured as s.t.p..

The outlet reaction mixtures were analysed on-line by gas chromatography equipped with a TCD detector (Varian-3900). Each analysis was repeated three times in order to minimize experimental error. Reaction measures in both SER and SEMR were carried out

after 10 min of stat running the WGS reaction, which ensures a maximum CO_2 adsorption in the hydrotalcite even if CO_2 sorption rate is slow. Moreover, in order to avoid the saturation of the hydrotalcite the feed mixture bypassed the reactor after testing each reaction temperature.

The CO conversion is defined as follows:

$$\text{CO}\ (\%) = \frac{F_{CO}^{In} - F_{CO}^{Out}}{F_{CO}^{In}} \times 100\% \quad (6)$$

Where F_{CO}^{In} and F_{CO}^{Out} represent the molar flow rates of CO in the feed and exit of the reactor, respectively. Both, sand F_{CO}^{Out} were measured on-line by using a gas chromatograph.

The H_2 and CO_2 yield is defined as follows:

$$\text{Y}_{\text{H2/CO}} = \frac{F_{H_2}^{Out}}{F_{CO}^{In}} \times 100\% \quad (7)$$

$$\text{Y}_{\text{CO2/CO}} = \frac{F_{CO_2}^{Out}}{F_{CO}^{In}} \times 100\% \quad (8)$$

Where $F_{H_2}^{Out}$, $F_{CO_2}^{Out}$ and F_{CO}^{Out} represent the molar flow ratesof H_2, CO_2 and CO at the exit of the reactor, respectively. All, $F_{H_2}^{Out}$, $F_{CO_2}^{Out}$ and F_{CO}^{Out} were measured on-line by using a gas chromatograph.

It should be noted that with the proposed definitions of the yields, based on the flow rate of the limiting reactant, and considered the stoichiometry of the WGSR (each mol of CO reacted yields one mole of H_2 and one mole of CO_2), the theoretical maximum value of the

sum of both yields is two. Obviously, both the reversibility of these reaction, the presence of side reaction (coking) and the CO_2 adsorption lead to significantly lower values.

3. Results and Discussion

In this work, the performance of the three catalytic reactors (FBR, SER and SEMR) during the WGS reaction has been studied. In order to compare their performance, all the catalytic activity tests were carried out under the same reaction conditions. A schematic representation of each reactor is shown in Figure 1.

1. Fixed-bed Reactor

The performance of the FBR was used as a reference for comparison with the results obtained in the SER and the SEMR.

Figure 2 shows CO conversion and H_2, CO_2, and C yields as a function of the temperature during the WGS reaction using a traditional FBR. It can be observed that CO conversion increased as the temperature increased reaching a maximum value of 62% at 350ºC after which point it decreased. This trend is well reported in the literature for exothermic equilibrium-limited reactions, where the rate of the reaction increases with temperature at the same time that the equilibrium constant decreases. The fact that CO conversion and H_2 and CO_2 yield curves fully fit each other in the temperature range studied indicates that no side reactions were observed and that the 10% CuO/CeO_2 catalyst was 100% selective to H_2 and CO_2. Indeed, Figure 2 shows that no C deposition was observed during the WGS reaction even at high temperatures.

2. Sorbent Enhanced Reactor

The performance of the SER, which consisted of a tubular reactor packed with an admixture of 10% CuO/CeO_2 catalyst and hydrotalcite-derived Mg-Al mixed oxide, was studied for the WGS reaction. Figure 3 shows the CO conversion and the H_2, CO_2 and C yields during the WGS reaction using the SER. It can be observed that the CO conversion in the SER increased as the reaction temperature increased reaching a plateau of 77 % at 360ºC, which differs from the CO conversion profile previously reported in the traditional FBR. In addition, the CO conversion in the SER is significantly larger that in a traditional FBR, (Figure 2). The removal of the CO_2 from the reaction medium by using the highly CO_2 selective hydrotalcite not only enhances the CO conversion but also overcomes the thermodynamic equilibrium limitation. Indeed, CO conversion at 360ºC is 77%, which is 23% higher than the thermodynamic equilibrium conversion and 33% higher than that in a traditional FBR. Similar results were observed by C. Han et al [39] and M.G. Beaver et al [40] but using CaO and Na_2O/Al_2O_3 as a CO_2 sorbent, respectively.

Nonetheless, it is important to note that CO conversion does not fit with the H_2 yield. This trend can be explained due to undesirable side reactions such as C deposition, which is favoured at high temperatures especially when the system is operated at low H_2O/CO ratios ($R \leq 1$). As is well known, Boudart (1) and CO reduction (2) reactions may become important at low H_2O/CO ratios [38].

$2CO \rightarrow CO_2 + C \qquad \Delta H = -173$ kJ/mol (1)

$CO + H_2 \rightarrow C + H_2O \quad \Delta H = -133$ kJ/mol (2)

Moreover, the presence of hydrotalcite could favour the formation and deposition of carbon at temperatures higher than 400ºC during the WGS reaction. Several examples of carbon deposition under different reaction conditions have been reported in the open

literature when Mg-Al mixed oxides are employed either as a catalyst or as a catalysts' support [42, 43]. J.I. Di Cosimo et al [44], found that an amount between 12-22 wt% of carbon was deposited over the Mg-Al mixed oxide surface during the acetone oligomerization reaction. K.Y. Koo et al [42], reported a deactivation of Ni/MgO-AlO_2 catalyst during the combined H_2O and CO_2 reforming of the CH_4 process (CSCRM) due to carbon deposition. In this respect, the acid-base surface properties of the Mg-Al mixed oxide determine not only the amount of carbon deposited but also its nature and composition [44]. Likewise, deactivation of the CuO/CeO_2 catalyst due to C deposition has also been reported in the literature. L. Yanyoung et al [45] observed that carbonaceous deposits formed on the CuO/CeO_2 catalysts' surface during the methanol steam reforming (MSR) reaction reduced the CH_3OH conversion by 20%. Moreover, P. Djinovićet al [46] found that during long-term stability tests of the CuO/CeO_2 catalyst during the WGS reaction, an amount of 0.34-0.39 wt% of coke was deposited over its surface.

Based upon this result, it seems that under these particular WGS reaction conditions the SER has an optimum window of operation between 300-400ºC. Nevertheless, C deposition could be avoided by either increasing the H_2O/CO ratio in the feed mixture, modifying the acid-base surface properties of hydrotalcite or by using a highly selective catalyst. According to the thermodynamic calculations performed by E. Xue et al [40], the catalyst deactivation due to C deposition can be easily avoided by increasing the H_2O/CO ratio ($R \geq 2$). At this point, it is important to note that hydrotalcites adsorb H_2O during their activation and operation, which could decrease the actual H_2O/CO ratio. Adsorption of H_2O on the surface of hydrotalcite-like compounds under industrial operating conditions [i.e., high temperatures (up to 450 ºC) at different partial water vapour pressures (from 0.0 to 2.5 atm) in multicomponent systems] has been studied by several authors [47-51]. However, the effect of

water vapour on the CO_2 capture capacity of hydrotalcites is still not clear. According to some authors [47, 48], the presence of water vapour has a negligible effect on the CO_2 capture capacity, whereas others [49-51] have reported that small amounts of water vapour significantly enhance it. The positive effect of water vapour on the CO_2 capture capacity of hydrotalcites could be due to several reasons. First, the presence of H_2O on the surface increases the potential energy of the hydrotalcite surface, which improves its CO_2 adsorption [52]. Second, water vapour not only maintains the hydroxyl concentration of the hydrotalcite surface, but also prevents its deactivation by coke deposition.

In order to better understand the role of the hydrotalcite-derived Mg-Al mixed oxide in the SER performance, the CO_2 balance during the WGS reaction was plotted in Figure 4A. It can be observed that the total CO_2 flow rate produced and the non-adsorbed CO_2 flow show a volcano curve profile with a maximum at 375ºC and 325ºC, respectively, whereas the adsorbed CO_2 shows a different curve profile. The CO_2 adsorption in the hydrotalcite-derived Mg-Al mixed oxide started at 150ºC and increased as the temperature is increased, reaching a plateau of 0.7 ml/min of CO_2 at 250ºC, after which it started increasing again at 325ºC as the temperature is increased and reaches to a maximum value of 1.3 ml/min at 375ºC, and then decreases as the temperature is further increased. This behaviour could be explained by an increase in the micro-porosity of the hydrotalcite at temperatures higher than 300ºC. According to Z. Yong et al [53], two different effects occur when the temperature increases that could affect the hydrotalcite CO_2 adsorption behaviour. In the temperature range from 100 to 300ºC, the interlayer d spacing of the hydrotalcite decreases when the temperature is increased due to H_2O desorption and consequently the amounts of CO_2 adsorbed on its surface decreases [54-56]. However, at temperatures higher than 300ºC the increase of the hydrotalcite micro-porosity due to both the dehydroxilation between OH groups of

continuous layers and the decarbonation process becomes the predominant effect, which significantly increases its CO_2 capacity [57]. Similar behaviour has been observed by Faba et al [58], who described the formation of different carbonate species due to the presence of sites with different basic strengths: bicarbonates (weak basic sites), bidentate carbonates (medium basic sites) and monodentate carbonates (strong basic sites). The desorption temperature of these species depends on their interaction with the sites and can rank as follow: bicarbonates (20 ºC < T < 100 ºC), bidentate carbonates (100 ºC < T < 300 ºC), and nonodentate carbonates (T > 300 ºC).

The percentage of CO_2 adsorbed on the hydrotalcite under the WGS reaction conditions is shown in Figure 4.B. Although hydrotalcites are able to capture about 1.9-5.2 wt% of CO_2 in a temperature range between 200 and 400ºC [47,48, 59], the percentage of CO_2 adsorbed did not reach 100% in the full temperature range studied. According to M. Leon et al [31], the CO_2 adsorption capacities of the hydrotalcite employed in this work is 0.84 mmol/g at 100ºC. The low percentage of adsorbed CO_2 cannot be justified by the saturation of the hydrotalcite as it is used in excess however, two different reasons can be discussed. Firstly, the CO_2 adsorption of the hydrotalcite is limited by its adsorption kinetics, which means that the whole exportation of the hydrotaltite required longer residence times. In this respect, B. Ficicilar et al [48] observed that the presence of steam decreases the sorption rate of CO_2 due to an increase of the diffusion resistance. Secondly, the amount of CO_2 adsorbed depends not only on the hydrotalcite properties but also on the CO_2 partial pressure along the reactor. M. Leon et al [37] has shown that at 50ºC the amount of CO_2 adsorbed on the hydrotalcite-derived Mg-Al mixed oxide increased from 0 to 0.4 mmol/g when the CO_2 pressure increased from 0 to 0.05 atm. As is well known, the SER, as well as traditional fixed-bed reactors, shows a linear CO_2 concentration gradient along the catalyst-sorbent packed bed during the

WGS reaction. Indeed, the CO_2 partial pressure in the first half part of the SER is very low, indicating that the CO_2 adsorbed in hydrotalcite is not important. This behaviour suggests a misuse of the hydrotalcite in the first half of the SER. In this respect a different configuration, such as placing hydrotalcite in the second half of the packed bed, could significantly improve the performance of the SER.

3. Sorbent Enhanced Membrane Reactor

The performance of the SEMR, which consists of a tubular reactor packed with an admixture of 10% CuO/CeO_2 catalyst and hydrotalcite-derived Mg-Al mixed oxide CO_2 sorbent within a Pd/Ag membrane, was studied during the WGS reaction. Figure 5 shows the CO conversion and the H_2, CO_2 and C yields during the WGS reaction using the SEMR. Undesirables side reactions (i.e. C deposition) can be observed at 300 ºC. This behaviour can be explained by two factors. Firstly, it is well-known that the H_2 permeation through the membrane increases the risk of C deposition, since the reaction medium atmosphere becomes more oxidant [60][61][62]. This agrees with the fact that C deposition and H_2 permeation through the Pd/Ag membrane began at the same reaction temperature. Secondly, as has been mentioned above, C deposition is favoured at high temperatures especially when the system is operated at low H_2O/CO ratios ($R \leq 1$). The combination of both an oxidant atmosphere and low H_2O/CO ratio could be the main reason for the large C deposition observed during the WGS reaction in the SEMR. In this respect, optimization of the SEMR can occur by increasing the H_2O/CO ratio and selecting the proper membrane thickness, which improve the reactor performance and minimises the potential of C deposition.

Figure 6 A-B shows the CO_2 balance and the percentage of CO_2 adsorbed on the hydrotalcite during the WGS reaction using the SEMR. It can be seen that the behaviour of

the hydrotalcite in the SEMR was very similar to that observed in the SER. Therefore, in this respect, the discussions made regarding the SER can be applied to the SEMR.

The performance of the Pd/Ag membrane in the SEMR during the WGS reaction is summarized in Figure 7A. It can be seen that H_2 permeation across the Pd/Ag membrane began at 200ºC and increased as the reaction temperature increased. The H_2 recovery index, i.e. H_2, permeated through the membrane and the total H_2 produced ratio is represented as a function of the reaction temperature in Figure 7B. This parameter is widely employed to study the efficiency of the Pd-based membrane under the reaction conditions in different membrane reactor designs. It can be seen in Figure 7B that the H_2 recovery increased lineally as the reaction temperature increased. This trend suggests that H_2 permeation across the Pd/Ag membrane is not limited by boundary layer or concentration polarization effects, and thus the H_2 is able to diffuse from the catalysts to the surface of the Pd/Ag membrane. However, competitive adsorption of CO, CO_2 and H_2O on the Pd/Ag surface can significantly decrease its H_2permeance [63-66].

In summary, these preliminary results show relevant data obtained using the SER and the SEMR, which allows for the better understanding and design of multifunctional catalytic hollow fibre reactors. It also points out that the growth of this technology needs a parallel development of; high active and stable catalysts, high H_2 permeable and selective membranes, fast capture/release kinetics and good mechanical strength CO_2 sorbent, advanced control strategy and engineering reactor design

4. Conclusion

The hydrotalcite-derived Mg-Al mixed oxide present in both SER and SEMR, enables the improvement of the H_2 production by in situ CO_2 capture during the WGS reaction.

Therefore, SER and SEMR allow the performance of the WGS reaction at lower temperatures or using lower amounts of catalyst. In addition, the SEMR combines the processes of generating and separating H_2 in a single step, which is possible due to the high selectivity of the Pd/Ag membrane, such that only H_2 produced during the reaction passes through it.

Nonetheless, that CO_2 recovery of hydrotalcite did not reach 100% either in the SER or SEMR, which could be explained due to both the high space velocity employed and the CO_2 concentration gradient formed along the packed bed during the WGS reaction. In this respect, an increase in the residence time and a different reactor configuration, like placing hydrotalcite in the second half of the packed bed, could significantly improve the performance of both the SER and SEMR.

Moreover, the combination of both oxidant atmosphere and low H_2O/CO ratio factor ($R \leq 1$) could be the main reason for the large C deposition observed during the WGS reaction using the SEMR. In this respect, the SEMR can be optimized by increasing the H_2O/CO ratio and selecting the proper membrane thickness, which improves the reactor performance and minimises the potential of C deposition.

Acknowledgements

The authors gratefully acknowledge the research funding provided by EPSRC in the United Kingdom (grant no. EP/G01244X/1).

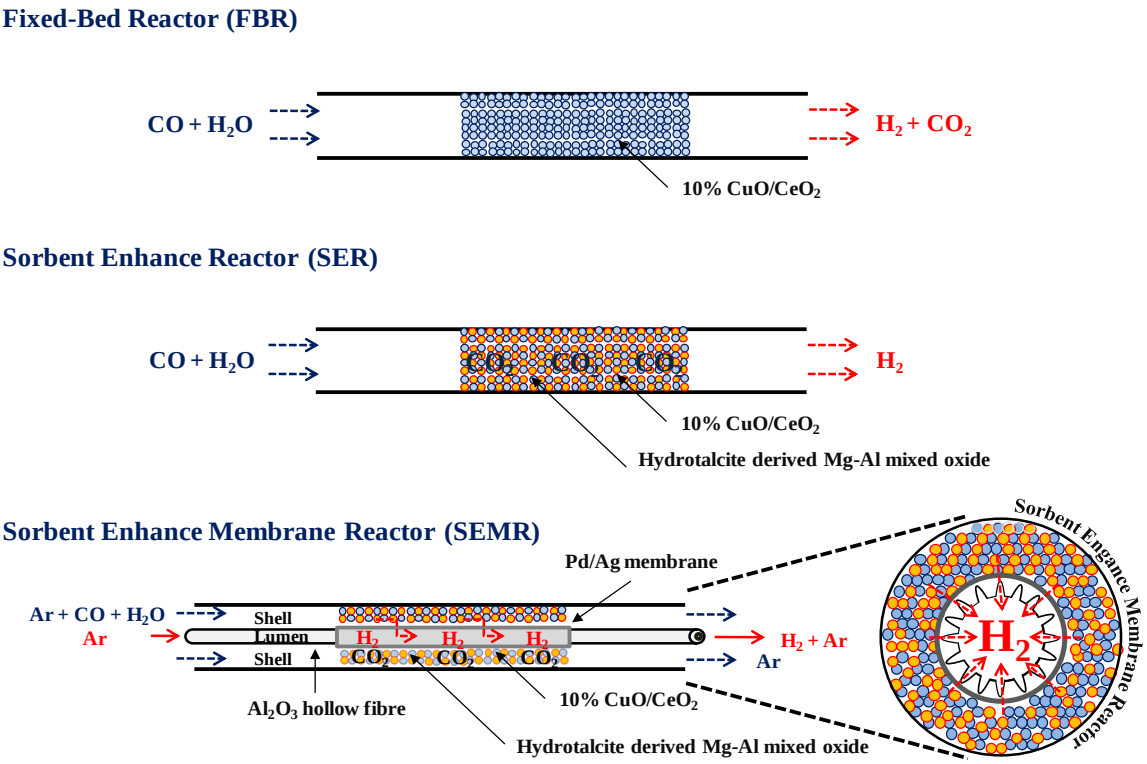

Figure 1: A schematic representation of the fixed-bed reactor (FBR), the sorbtion enhanced reactor (SER) and the sorption enhanced membrane reactor (SEMR).

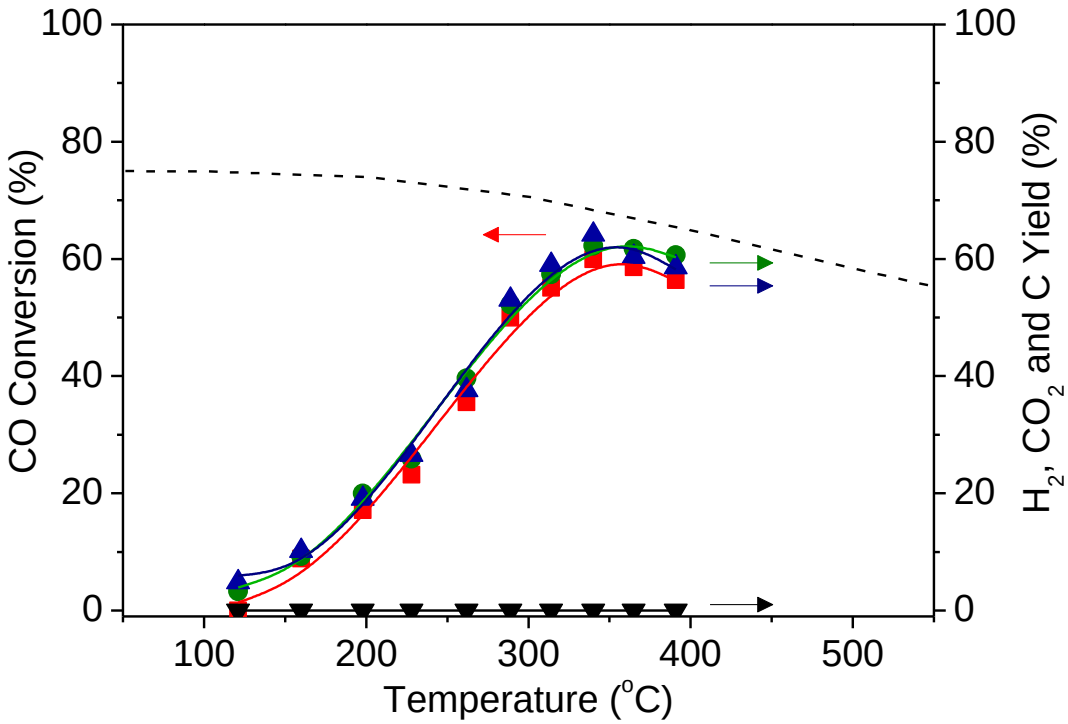

Figure 2. CO conversion (■), and H_2 (●), CO_2 (▲), and C (▼) yields(based on the CO inlet molar flow rate) as a function of the temperature during the WGS reaction using a traditional fixed-bed reactor.

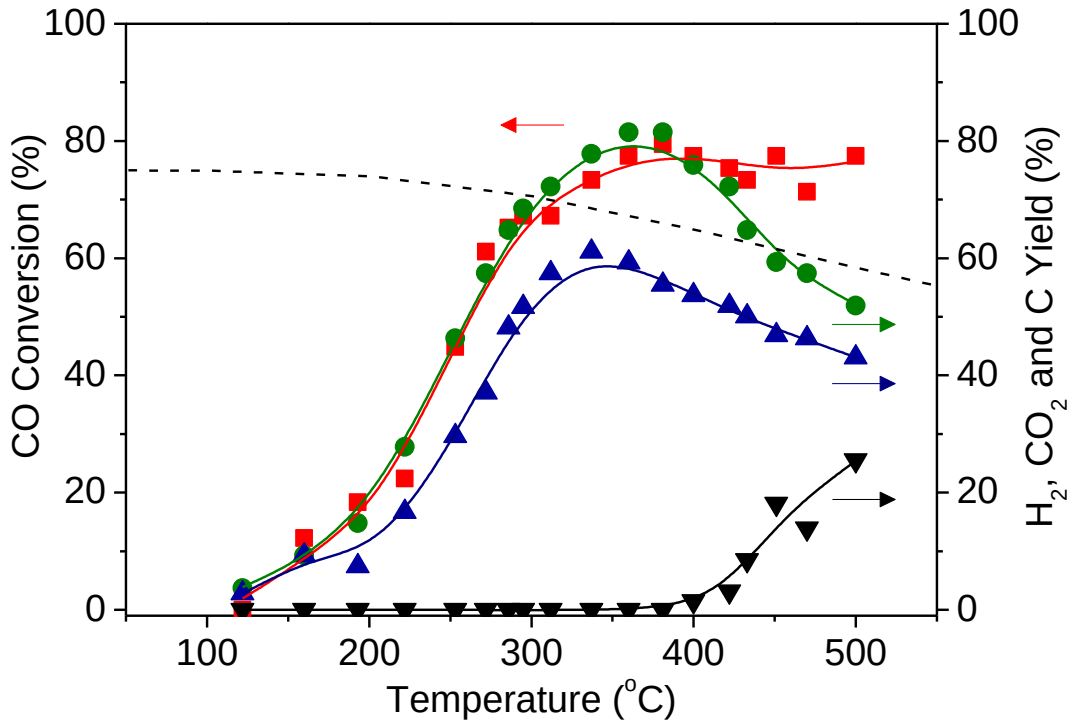

Figure 3.CO conversion (■), and H_2 (●), CO_2 (▲), and C (▼) yields(based on the CO inlet molar flow rate) as a function of the temperature during the WGS reaction using a sorbtion enhanced reactor.

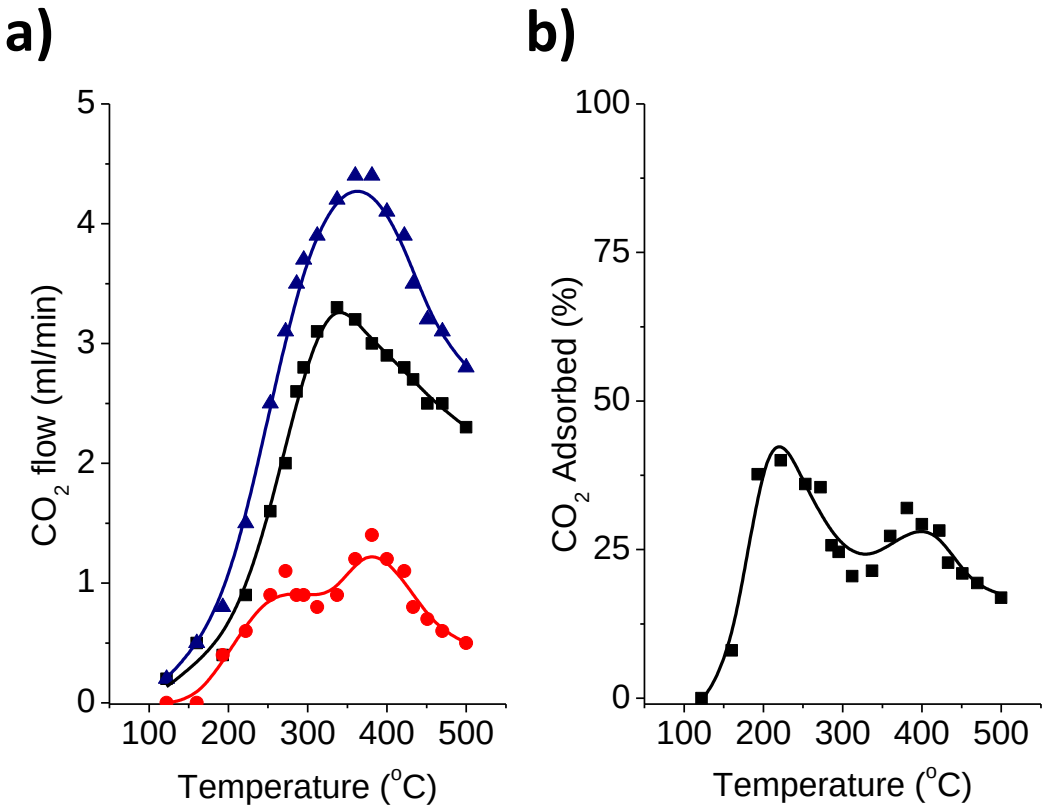

Figure 4. (a) CO_2 production as a function of the temperature during the WGS reaction using a sorbtion enhanced reactor: total (▲), unadsorbed (■), and adsorbed (●). (b) CO_2 recovery as a function of the temperature during the WGS reaction using hydrotalcite. Volumetric flow rates are measure at standard conditions ($P=10^5$ Pa, T=273 K)

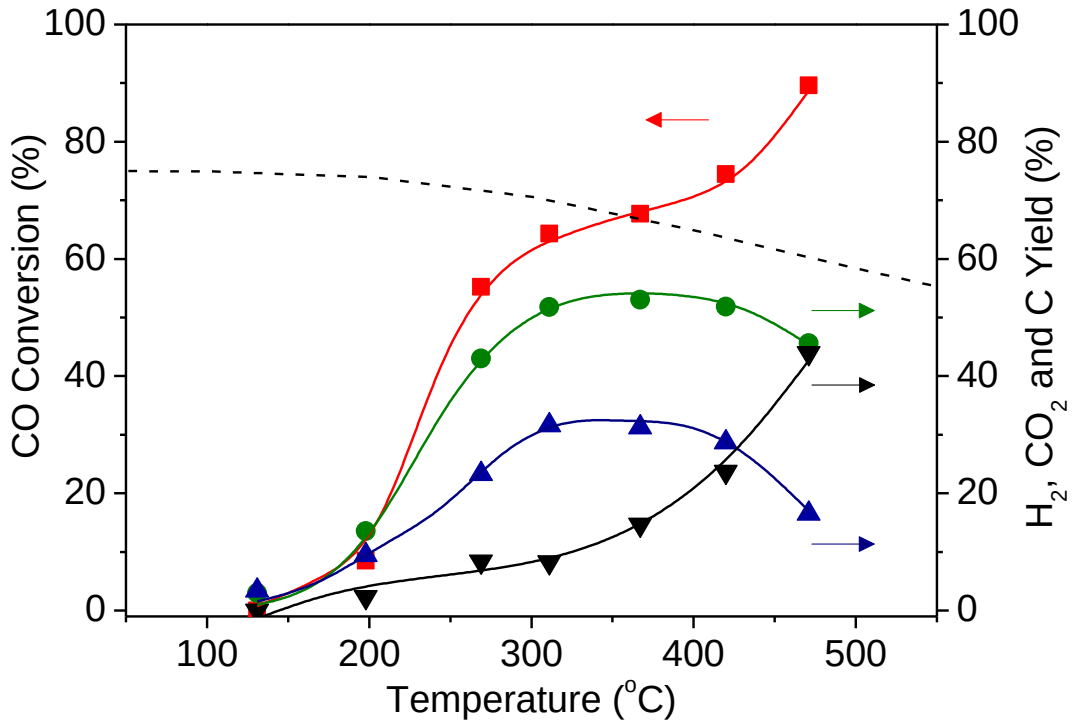

Figure 5. CO conversion (■), and H_2 (●), CO_2 (▲), and C (▼) yields (based on the CO inlet molar flow rate) as a function of the temperature during the WGS reaction using a sorbtion enhanced membrane reactor.

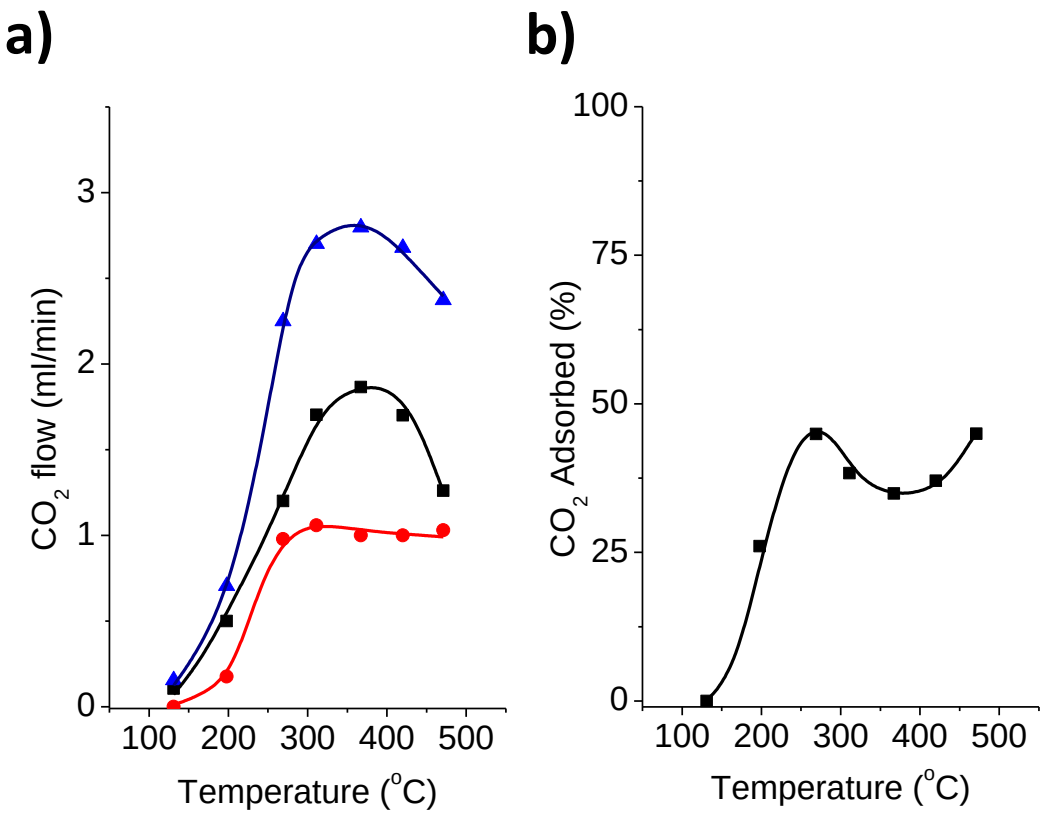

Figure 6. (a) CO_2 production as a function of the temperature during the WGS reaction using a sorbtion enhanced membrane reactor: total (▲), unadsorbed (■), and adsorbed (●). (b) CO_2 recovery as a function of the temperature during the WGS reaction using hydrotalcite.. Volumetric flow rates are measure at standard conditions (P=10^5 Pa, T=273 K)

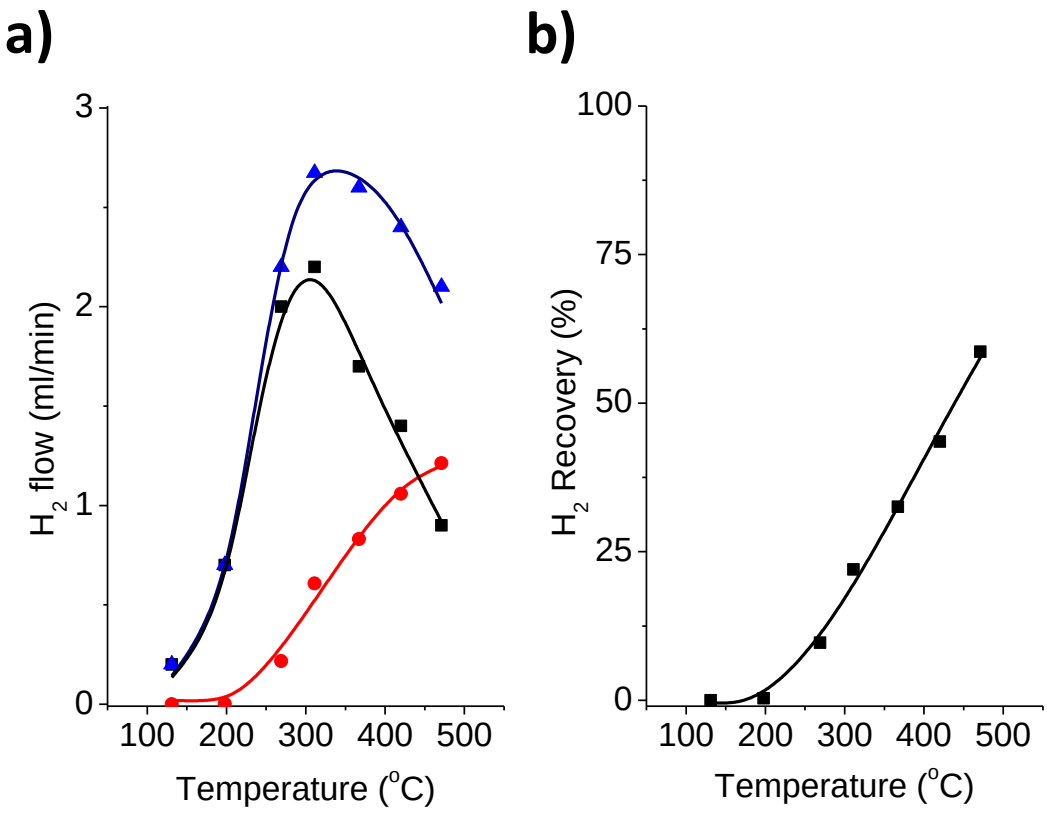

Figure 7. (a) H_2 production as a function of the temperature during the WGS reaction using a sorbtion enhanced membrane reactor: total (▲), retained (■), and permeated (●). (b) H_2 recovery as a function of the temperature during the WGS reaction using a Pd/Ag membrane. Volumetric flow rates are measure at standard conditions ($P=10^5$ Pa, T=273 K)

References

[1] L.O. Williams, Appl. Energ. 23 (1986) 171-178.
[2] A. Midilli, M. Ay, I. Dincer, M.A. Rosen, Renew. Sust. Energ. Rev. 9 (2005) 255-271.
[3] N.Z. Muradov, T.N. Veziroglu, Int. J. Hydrogen Energ. 30 (2005) 225-237.
[4] M. Momirlan, T.N. Veziroglu, Int. J. Hydrogen Energ. 30 (2005) 795-802.
[5] Chemical Economics Handbook, SRI - July 2001.

[6] Industrial Gases by the Chemical Economics Handbook, SRI – October 2007
[7] P. Marin, S. Ordóñez, F.V. Díez, Int. J. Hydrogen Energ.37 (2012) 4997-5010
[8] K.B. Lee, M.G. Beaver, H.S. Caram, S. Sircar, Ind. Eng. Chem. Res.47 (2008) 8048-8062.
[9] Catal. Today 156 (2010) 75-322.
[10] Catal. Today 104 (2005) 101-371.
[11] F.R. García-García, B.F.K. Kingsbury, M.A. Rahman, K. Li. Catal. Today 193 (2012) 20-30.
[12] F.R. García-García, M.A. Soria, C. Mateos-Pedrero, A. Guerrero-Ruiz, I. Rodríguez-Ramos, K. Li. J. Membr. Sci. 435 (2013) 218-225.
[13] F.R. García-García, K.M.K.Yu, S.C. Tsang, K. Li. Promedia Engineering 44 (2012) 191-193.
[14] F.R. García-García, L. Torrente-Murciano, D. Chadwick, K. Li. J. Membr. Sci. 405-406 (2012) 30-37.
[15] D.T. Hughes, I.R. Harris, J. Less, Common Metals 61(1978) 9-21.
[16] D. Wang, T.B. Flanagan, K.J. Shanahan, J. Phys. Chem. B, 2008, 112 1135.
[17] C.C. Koch, Nanostructured materials; processing, properties and potential applications. William Andrew Publishing/Noyes.
[18] J. Okazaki, D.A. Pacheco Tanaka, M.A. Llosa Tanco, Y. Wakui, F. Mizukami, T.M. Suzuk, J. Membr. Sci. 282 (2006) 370-374.
[19] S.N. Paglieri, J.D. Way. Innovation on palladium membrane research. Sep. Purif. Methods 3 (2002) 1–169.
[20] W. Gluud, K. Keller, R. Schonfelder, W. Klempt, U.S. Patent No.1,816,523 (1931).
[21] A.M. Squires, Adv. Chem. Ser. 69 (1967) 205-229.
[22] J.R. Hufton, S. Mayorga, S. Sircar, AIChE J., 45 (1999) 248–256.
[23] S. Sircar, J.R. Hufton, S. Nataraj, U.S. Patent No. 6,103,143 (2000).
[24] M. León, E. Díaz, A. Vega, S. Ordóñez, Chem. Eng. J. 175 (2011) 341-348
[25] S. Choi, J.H. Drese, C.W. Jones, ChemSusChem, 2 (2009) 796-854.
[26] D.S. Newsome, Catal. Rev. Sci. Eng.21 (1980) 275-318.
[27] B. Park, Ph.D. Thesis, University of Southern California, Los Angeles, CA, 2001
[28] S.Y. Lim, B. Park, F. Hung, M. Sahimi, T.T. Tsotsis, Chem. Eng. Sci. 57 (2002) 4933-4946.
[29] B. Park, T.T. Tsotsis, Chem. Eng. Proc. 43 (2004) 1171–1180.
[30] B. Park, Korean J. Chem. Eng. 21 (2004) 782-792.
[31] M. León, E. Díaz, S. Bennici, A. Vega, S. Ordóñez, A. Auroux, Ind. Eng. Chem. Res. 49 (2010) 3363-3671
[32] Z. Chen, S.S.E.H. Elnashaie, Ind. Eng. Chem. Res. 43 (2004) 5449-5459
[33] P. Prasad, S.S.E.H. Elnashaie, Ind. Eng. Chem. Res. 43 (2004) 494-501.
[34] P. Prasad, S.S.E.H Elnashaie, Ind. Eng. Chem. Res. 42 (2003) 4715–4722.
[35] Z. Chen, Y. Yan, S.S.E.H. Elnashaie, Chem. Eng. Sci. 58 (2003) 4335-4349.
[36] F.R. García-García, M.A. Rahman, I. D. González-Jiménez, K. Li. Catal. Today171 (2011) 815-821.
[37] B.F.K. Kingsbury, K.Li, J. Membr. Sci. 328 (2009) 134-140.
[38]J.N. Keuler, L. Lorenzen, R.D. Sanderson, V. Prozesky, W.J. Przybylowicz, Thin Solid Films 347 (1999) 91-98.
[39] C.Han, D.P. Harrison, Chem. Eng. Sci. 49 (1994)5875-5883.
[40] M.G. Beaver, H.S. Caram, S. Sircar, Int. J. Hydrogen Energ. 34 (2009) 2972-2978.
[41] E. Xue, M. O'Keeffe, J.R.H. Ross, Catal. Today. 30 (1996) 107-118.

[42] K.Y. Koo, H.S. Roh, U.H. Jung, D.J. Seo, Y.Seo, W.L. Yoon, Catal. Today. 146 (2009) 166-171.
[43] V.K. Díez, C.R. Apesteguía, J.I. Di Cosimo, Latin Am. Appl. Res. 33 (2003) 79-86.
[44] J.I. Di Cosimo, V.K. Diez, M. Xu, E. Iglesia, C.R. Apesteguia, J. Catal. 178 (1998) 499-510.
[45] L. Yanyong, H. Takashi, S. Kunio, H. Satoshi, T. Tatsuo Tsunoda, I. Tomoko, K. Mikio, ApplCatal A: Gen. 223 (2002) 137–145.
[46] P. Djinović, J. Batista, A. Pintar, Catal. Today. 147 (2009) S191-S197
[47] Y. Ding, E. Alplay, Chem. Eng. Sci. 55 (2000) 3461-3474.
[48] B. Ficicilar, T. Dogu, Catal. Today 115 (2006) 274-278.
[49] H.Th.JReijers, S.E.A. Valster-Schiermeier, P.D. Cobden, R.W. Van den Brink, Ind. Eng. Chem. Res. 45 (2006) 2522–2530.
[50] Z. Yong, A.E. Rodriguez, Energ. Convers. Manage. 43 (2002) 1865–1876.
[51] S. Choi, J.H. Drese, C.W. Jones, ChemSusChem 2 (2009) 796–854
[52] J. Wang, A.G. Kalinichev, R.J. Kirkpatrick, X. Hou, HydrationChem. Mater.13 (2001)145–150
[53] Z. Yong, V. Mata, A.E. Rodrigues, Ind. Eng. Chem. Res.40 (2001)204–209
[54] M. Gang, M Tsuji, Y Tamaura, Clays Clay Miner. 41 (1993) 731-737.
[55] F. Rey,V. Fornes, J. Chem. Soc., Faraday Trans. 88 (1992) 2233-2238.
[56] B. Maurizio, B. Rebours, O. Clause, J. Lynch, D. Bazin, E. Elkaım, J. Phys. Chem. 100 (1996) 8535-8542.
[57] L. Faba, E. Díaz, S. Ordóñez,Applied Catal. B, 113–114 (2012) 201-211
[58] Y. Ding, E. Alpay, Process Safety and Environmental Protection 79 (2001) 45-51.
[59] K. Hou, M. Fowles, R. Hughes,Chem. Eng. Sci.54 (1999) 3783–3791.
[60] M.N. Pedernera, J. Piña, D.O. Borio, J.Chem. Eng.134 (2007)138–144.
[61] R. Schafer, M. Noack, P. Kolsch, M. Stohr, J. Caro, Catal. Today82 (2003)15–23.
[62] M.P. Gimeno,Z.T. Wu, J. Soler, J. Herguido, K. Li, M. Menéndez,J.Chem. Eng. 155 (2009) 298-303.
[63] G. Barbieri, F. Scura, F. Lentini, G. De Luca, E. Drioli, Sep. Purif. Technol. 61 (2008) 217-224.
[64] A.L. Augustine, Y.H. Ma, N.K. Kazantzis, Int. J. Hydrogen Energ. 36 (2011) 5350-5360.
[65] Israni, S.H.; Harold, M.P. Ind. Eng. Chem. Res. 49 (2010) 10242-10250.
[66] D. Mendes, A. Mendes, L.M. Madeira, A. Lulianelli, J.M. Sousa, A. Basile, Asia-Pac. J. Chem. Eng.5 (2010) 111-137.